Direct Measurement of Gas Solubilities in Polymers with a High-Pressure Microbalance

N. von Solms,[1] J. K. Nielsen,[2*] O. Hassager,[2] A. Rubin,[3] A. Y. Dandekar,[1†] S. I. Andersen,[1] E. H. Stenby[1]

[1]*Centre for Phase Equilibria and Separation Processes (IVC-SEP), Department of Chemical Engineering, Technical University of Denmark, DK-2800 Lyngby, Denmark*
[2]*Danish Polymer Centre, Department of Chemical Engineering, Technical University of Denmark, DK-2800 Lyngby, Denmark*
[3]*NKT Fliexibles I/S, Priorparken 880, DK-2605 Brøndby, Denmark*

Received 18 October 2002; accepted 17 June 2003

ABSTRACT: Solubility and diffusion data are presented for methane and carbon dioxide gases in high-density polyethylene. The polymer was cut from extruded piping intended for use in offshore oil and gas applications. The measurements were carried out with a high-pressure microbalance. The properties were determined from 25 to 50°C and from 50 to 150 bar for methane and from 20 to 40 bar for carbon dioxide. In general, a good agreement was obtained with similar measurements reported in the literature. The solubility followed Henry's law (linear) dependence with pressure, except at high pressures for methane, for which negative deviations from Henry's law behavior were observed. The diffusion coefficients for each of the gases in the polymer were also measured with the balance, although the uncertainty was greater than for the solubility measurements. © 2003 Wiley Periodicals, Inc. J Appl Polym Sci 91: 1476–1488, 2004

Key words: gas permeation; polyethylene (PE); solution properties

INTRODUCTION

The offshore oil and gas industry is increasingly turning to the use of flexible flow lines and risers for the development of marginal fields in mature regions and in locations without an established infrastructure. A flexible flow line typically consists of inner and outer polymer tubes (an inner lining and an outer sheath, usually not of the same material) separated by helically wound steel armor. In oil-drilling operations, materials must be able to withstand drilling mud, acid water, and hydrocarbon liquids and gases at pressures up to 1000 bar and temperatures ranging from 4°C in the deep sea to 180°C in some North Sea wells. The inner liner needs to be resistant to the passage of such gases as carbon dioxide, methane, and hydrogen sulfide, whereas the outer sheath must protect the annulus from seawater and mechanical impact.[1,2]

The susceptibility of a polymer to penetration by a gas is determined by its permeability. However, permeability is a two-step process, involving both the solution of the gas in the polymer and the diffusion of the gas through the polymer.[3] To understand the mechanisms of gas permeation through a polymer membrane, we must understand both of these processes. In this work, we consider primarily the solution process. We measure the solubility of the gases carbon dioxide and methane in high-density polyethylene (HDPE) cut from flexible piping intended for offshore use over a range of temperatures and pressures (see the Experimental section).

The transport and thermodynamic properties of gases in polymers have been studied for a long time, with industrial interest dating back to the widespread use of the motor car tire.[4,5] However, the study of polymer films as barriers to gas transport was put on a firm scientific footing with the publication of a series of articles by Michaels and coworkers.[6–9] They examined both solubility and diffusion in polyethylene for various gases, including carbon dioxide, although their studies were limited to low pressures. In general, gas solubility is derived from dynamic studies, in which the gas permeability and diffusion are measured and the solubility is then derived from these properties. Michaels and Bixler[8] reported an early use of a direct solubility measurement, similar to that employed here, which greatly increased the accuracy of the value obtained. Similar measurements were also reported by Lowell and McCrum[10] and Kulkarni and

Correspondence to: E. H. Stenby (ehs@kt.dtu.dk).
**Present address:* Danish Metrological Institute, DK-2100 Copenhagen, Denmark.
† *Present address:* Department of Petroleum Engineering, University of Alaska, Fairbanks, Alaska 99775.
Contract grant sponsor: Danish Energy Research Program.

Journal of Applied Polymer Science, Vol. 91, 1476–1488 (2004)

Stern.[11] Aubert[12] described the use of a quartz microbalance for the determination of the solubilities of carbon dioxide in various polymers. Webb et al.[13] studied the effect of the draw ratio on the transport properties of gases in polyethylene. The solubility was determined with a dynamic technique.

With the measurements obtained from our apparatus, diffusion coefficients can also be determined. The method used to calculate the diffusion coefficients and the diffusion coefficients obtained are reported in this article.

This article is arranged as follows. First, there is a discussion of the materials and experimental procedure. Then, the solubility and diffusion results are given for the systems studied. The required theoretical background is developed both in this section and in the discussion of the experimental procedure. Finally, some conclusions based on the work are drawn.

EXPERIMENTAL

The HDPE samples used in the study were discs machined from extruded polymer piping intended for use. The reported density of the originally supplied polymer was 0.954 g/cm^3. The extruded samples used in the study were determined by us to have a density of 0.955 g/cm^3. The discs were approximately 10 mm in diameter and 0.5 mm thick. Enough discs were used to make up a polymer mass of about 0.3 g (usually eight discs). The weight of the polymer was balanced by small quartz spheres on the opposite arm of the balance. The density of the quartz spheres was measured to be 2.65 g/cm^3. Methane and carbon dioxide gas samples were supplied in industrial gas bottles by Air Liquide (Ballerup, Denmark). The purity of the gas samples was greater than 99.99%.

A schematic diagram of the apparatus used to perform the solubility measurements is shown in Figure 1. The high-pressure balance was an S3D-P instrument provided by Sartorius AG (Göttingen, Germany). The operating limits of the balance were temperatures ranging from 0–150°C and pressures up to 150 bar. The weighing limit was 100 mg. The weighing beam was located in the weighing cell enclosed by a pair of metallic slabs. The ends of the beam were connected to quartz weighing pans by wire hangers located in the pressure tubes. The measured mass was accurate to $\pm$0.001 mg. The weighing beam was calibrated with 50- and 100-mg CuNi18Zn20 calibration weights certified to ± 2 μg by Sartorius. An Entran pressure transducer measured the pressure in the pressure tubes and weighing chambers to $\pm$0.1 bar. The temperature was maintained by the submersion of the weighing chambers in glycerin in a jacketed and insulated tank, with glycerin circulated through the jacket. The temperature was kept constant with an automatic controller.

Figure 2 shows sample pressurization and evacuation runs for methane in HDPE at 32°C and 55.5 bar. A pressurization run was followed by an evacuation run to yield two weight measurements at each pressure. For about half of the experiments, this process was performed twice to yield four weight measurements at each pressure. The weight measurements were allowed to equilibrate for 30–48 h, depending on the pressure, until no further increase (pressurization) or decrease (evacuation) was observed. An experiment was started by the evacuation of the balance to remove any gases that may have been adsorbed at the ambient pressure. The cell was then pressurized rapidly up to the desired experimental pressure, and the polymer weight and time were logged initially every 2 s and then after about 5 min every 20 s. After the completion of a pressurization run (30–48 h), once the polymer weight was equilibrated, an evacuation run commenced. The balance was rapidly evacuated, and the gas then started to desorb from the polymer. As can be seen in Figure 2, immediately upon pressurization, the polymer mass apparently dropped dramatically. This was an effect of buoyancy: the polymer seemed lighter in the dense gas. In general, this phenomenon had no effect on the experiment because the true zero (the minimum of the pressurization curve or the maximum of the evacuation curve) could be observed from the readings. However, in the few cases in which the pressurization or evacuation was not performed rapidly enough, or in which instability immediately upon a change in the pressure made the zero difficult to ascertain, the zero was calculated by correction for buoyancy. The accuracy of this calculation was established by the fact that the results were in agreement with the observed zero for the majority of the runs. The sample calculation of the buoyancy correction is given next. The calculation was performed for the pressurization case of Figure 2. Immediately upon pressurization, both arms of the balance were buoyed upward by the denser gas. The apparent mass change of the polymer is

$$\Delta m_p = \frac{m_p}{\rho_p}(\rho_p - \rho_M) - m_p \tag{1}$$

where m_P and ρ_P are the true mass and density of the polymer, respectively, and ρ_M is the density of the gas (methane, in this case). The apparent mass change of the glass beads is

$$\Delta m_G = \frac{m_G}{\rho_G}(\rho_G - \rho_M) - m_G \tag{2}$$

where m_G and ρ_G are the true mass and density of the glass, respectively. The change in the instrument reading (Δm_I) is then

$$\Delta m_I = \Delta m_G - \Delta m_P = \rho_M \left(\frac{m_P}{\rho_P} - \frac{m_G}{\rho_G}\right) \tag{3}$$

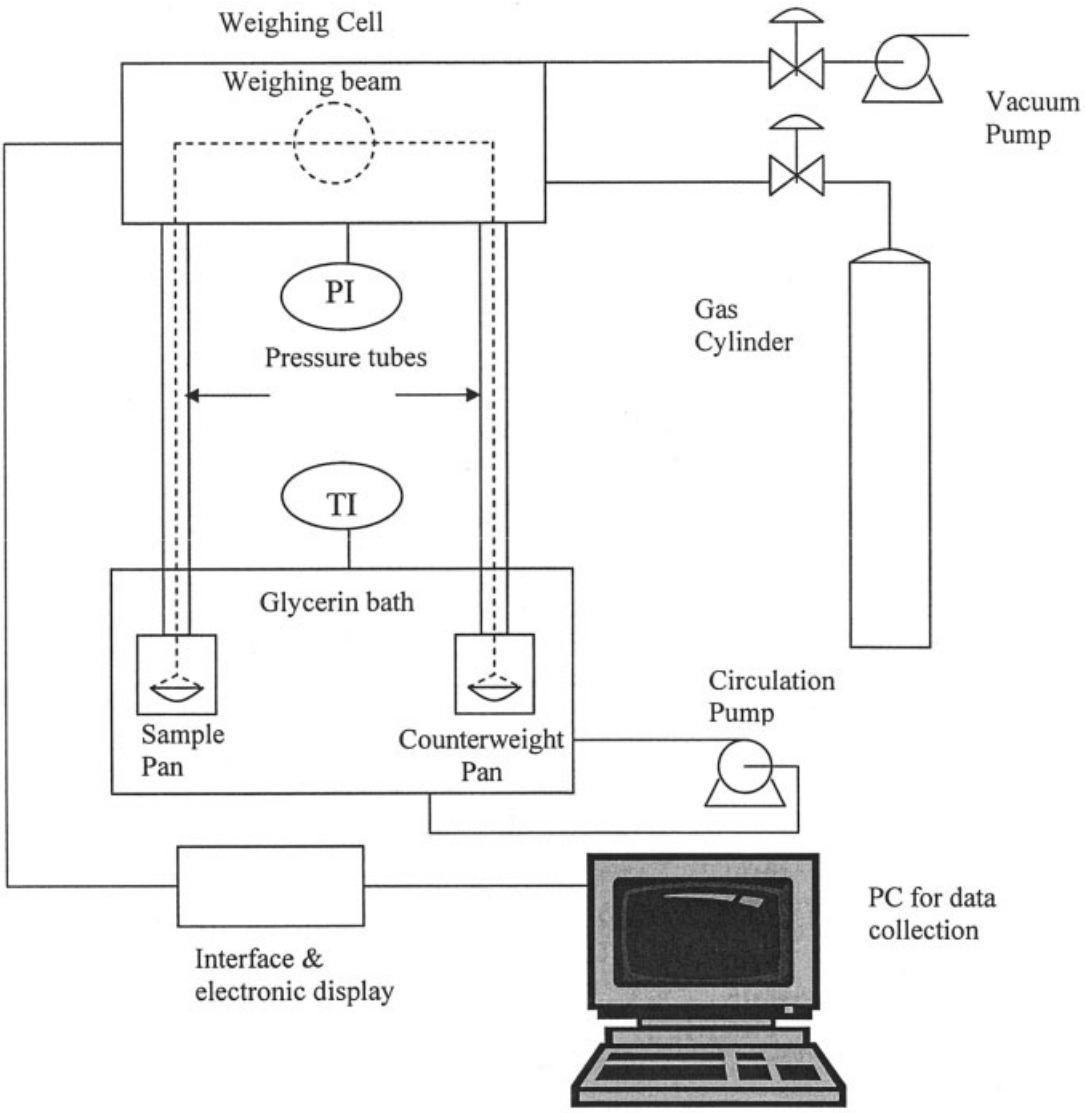

Figure 1 Schematic diagram of the high-pressure balance apparatus used to measure the gas solubility in the polymers.

For the pressurization run of Figure 2, inserting the values $\rho_M = 0.0383$ g/cm^3, $\rho_P = 0.955$ g/cm^3, $\rho_G = 2.65$ g/cm^3, $m_P = 0.3252$ g, and $m_G = 0.2964$ g, we obtained $\Delta m_I = 8.76$ mg. Thus, the instrument reading was predicted to jump from 46.69 to 55.45 mg. This agreed with the observed value of 55.49 mg.

Solubility experiments were performed for the two pure gases, methane and carbon dioxide, in HDPE. For each of the two gases, the runs were performed at four temperatures: 25, 32, 40, and 50°C. For methane, the experiments were carried out around 50, 100, and 150 bar; for carbon dioxide, they were carried out at 20, 30, and 40 bar.

Gas densities over the pressure and temperature ranges were obtained from a modified Benedict–Webb–Rubin equation of state, the parameters of which were obtained from pressure–volume–temperature (P–v–T) measurements up to 1000 bar.[14] The agreement with the experimental density data was better than 0.1% over the whole range. Pure gas densities obtained from this equation of state within the range of applicability may be considered to be pseudoexperimental data.

RESULTS AND DISCUSSION

Gas solubility

Figures 3 and 4 show the measured solubilities as grams of gas per gram of polymer for the two systems: methane/HDPE (Fig. 3) and carbon dioxide/HDPE (Fig. 4). The values are also tabulated in Tables I and II. The solubilities of both gases increase with pressure and decrease with temperature, although the temperature effect is not as pronounced. As the methane pressure increases above about 100 bar in Figure 1, the

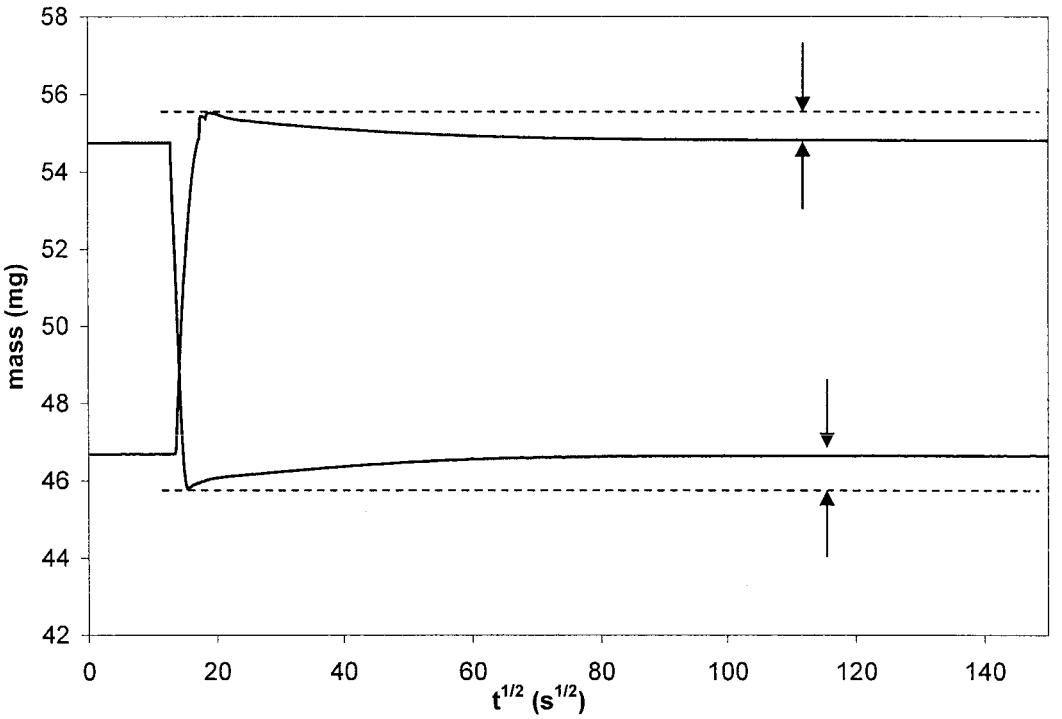

Figure 2 Pressurization and evacuation experiments for methane in HDPE at 55.5 bar and 32°C. The polymer mass is plotted against the square root of time. The difference between the initial and final masses of the polymer is the amount of gas absorbed or desorbed.

pressure dependence becomes nonlinear (there are deviations from Henry's law behavior). However, in the carbon dioxide/HDPE system (Fig. 4), for which the pressure is less than 40 bar, no such deviations from linearity can be observed. Pressures were necessarily kept low in this system to prevent liquefaction of carbon dioxide. It is interesting and instructive to compare our data with similar data available in the literature. Chau and Raspor[15] measured gas diffusivities and permeabilities for methane and carbon dioxide in HDPE. From these measurements, they calculated the solubility indirectly:

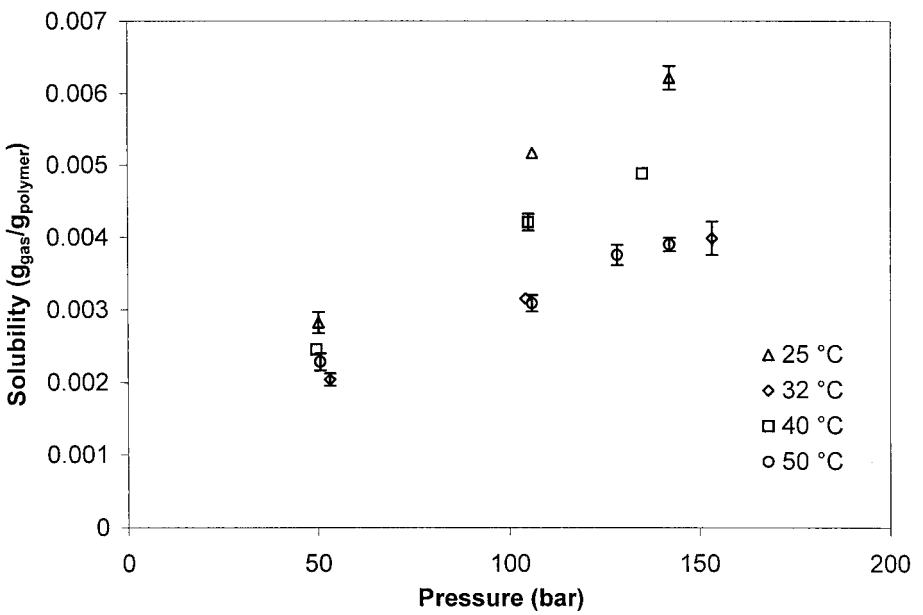

Figure 3 Solubility of methane in HDPE as a function of pressure at different temperatures.

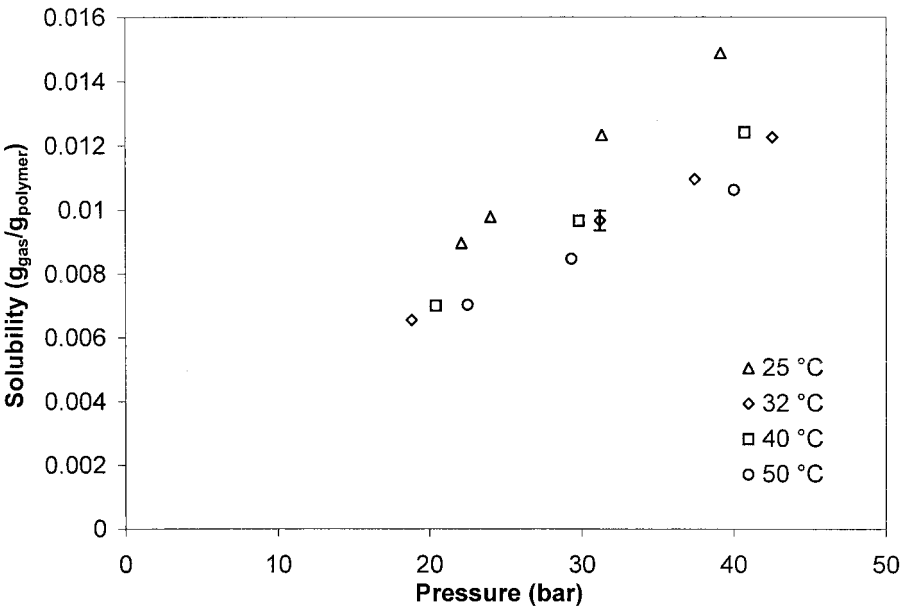

Figure 4 Solubility of carbon dioxide in HDPE as a function of pressure at different temperatures.

$$P = SD \tag{4}$$

where P is the gas permeability [cm^3(STP) cm/cm^2 s atm], D is the gas diffusivity (cm^2/s), and S is the solubility [cm^3(STP)/cm^3 atm]. The uncertainty in this method is increased by the fact that the diffusivity must also be measured with, for example, the time-lag method.[16] The focus of that study was to examine the effect of the orientation of polymer molecules on the gas-transport properties. Polymer molecules were oriented by the drawing (stretching) of the polymer to various extents. They did, however, report data for an undrawn polymer, with which we compare our results. Figure 5 shows a comparison of our results at 25°C with their results at 23.2°C. Because they did not report the pressures at which their experiments were carried out, their single data point for each gas/polymer pair appears as a line, converted into our solubility units of grams of gas per gram of polymer. The agreement between the two sets of data is good, although it is clear that our data are nonlinear (i.e., they deviate from Henry's law behavior). Unfortunately, the pressure at which the permeation experiments of Chau and Raspor[15] were performed was not reported,

TABLE I
Solubilities of Methane in HDPE

25°C		32°C		40°C		50°C	
Pressure (bar)	Solubility (g of gas/g of polymer) $\times 10^3$	Pressure (bar)	Solubility (g of gas/g of polymer) $\times 10^3$	Pressure (bar)	Solubility (g of gas/g of polymer) $\times 10^3$	Pressure (bar)	Solubility (g of gas/g of polymer) $\times 10^3$
50.1	2.97	48.3	1.97	49.6	2.45	50.2	2.18
50.1	2.68	55.5	2.16	49.6	2.46	50.2	2.24
		55.5	1.99			50.9	2.21
						50.9	2.48
106	5.18	103.8	3.24	105	4.29	105.4	3.74
106	5.15	103.8	3.12	105	4.13	105.4	3.58
		105	3.11			106.3	3.89
						106.3	3.81
142.2	6.05	150	3.58	135.2	4.86	128.6	3.98
142.2	6.38	151	4.11	135.2	4.92	128.6	4.26
		151	4.21			142.2	4.24
		157.1	4.15			142.2	4.42
		157.1	3.9				

Pressure was either pressure applied during a pressurization run or equilibrium pressure immediately preceding an evacuation run.

TABLE II
Solubilities of Carbon Dioxide in HDPE

25°C		32°C		40°C		50°C	
Pressure (bar)	Solubility (g of gas/g of polymer) $\times 10^3$	Pressure (bar)	Solubility (g of gas/g of polymer) $\times 10^3$	Pressure (bar)	Solubility (g of gas/g of polymer) $\times 10^3$	Pressure (bar)	Solubility (g of gas/g of polymer) $\times 10^3$
22.1	8.92	18.8	6.53	20.4	6.90	22.5	7.00
22.1	9.02	18.8	6.58	20.4	7.11	22.5	7.05
24	9.73						
24	9.85						
31.3	12.3	29.9	9.55	29.8	9.65	29.3	8.56
31.3	12.4	31.4	9.14	29.8	9.68	29.3	8.38
		31.4	9.79				
		31.6	10.0				
		31.6	9.89				
39.1	14.9	37.4	11.0	40.7	12.5	40	10.6
39.1	14.9	42.5	12.2	40.7	12.3	40	10.6
		42.5	12.3				

Pressure was either pressure applied during a pressurization run or equilibrium pressure immediately preceding an evacuation run.

but it was probably low. Their experiments were carried out at 23.2°C. The density of the undrawn polymer was 0.9577 g/cm^3. Figure 6 shows the corresponding plot for carbon dioxide. Clearly, both data sets were linear with the pressure, although Chau and Raspor measured a solubility lower than what we have measured. Because they used the same polymer for both gas permeability measurements, this further suggests that the pressure at which they performed the methane permeability measurements was low.

The data of Flaconnèche et al.[17] shown in Figure 7 present similar trends and magnitudes for two different samples of HDPE. The samples used in that study had densities higher (a high crystallinity HDPE that the authors call HDPE-R1, $\rho = 0.978$ g/cm^3) and lower (HDPE, $\rho = 0.943$ g/cm^3) than that used in this study. Their measured solubilities showed little variation with the temperature. However, the data sets obtained for each polymer sample effectively bracket our measurements; this is to be expected because the gas solubility tends to increase with decreasing polymer density. This group also inferred solubility indirectly from permeation measurements with eq. (4). Unfortunately their measurements were limited to 100 bar, so it is not

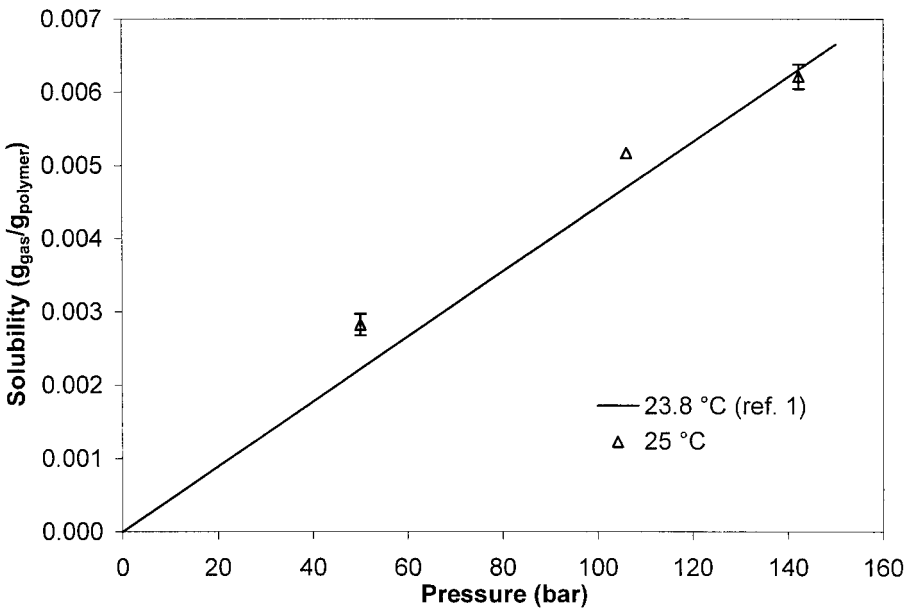

Figure 5 Solubility of methane in HDPE as a function of pressure. The straight line represents the data of Chau and Raspor[15] converted into this study's units.

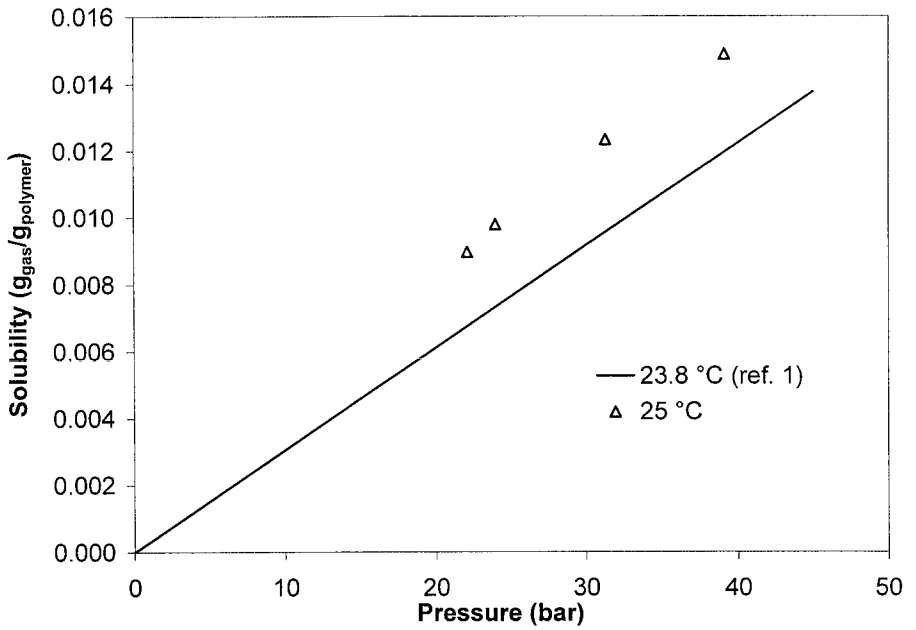

Figure 6 Solubility of carbon dioxide in HDPE as a function of pressure. The straight line represents the data of Chau and Raspor[15] converted into this study's units.

clear from their study whether deviations from Henry's law can be deduced. Figure 8 presents the corresponding comparison for the carbon dioxide/HDPE system. The sparseness of data from Flaconnèche et al.[17] makes it difficult to draw any clear comparisons, although certainly the solubilities are of approximately the same magnitude. Our data at 40°C are comparable to the lower density polyethylene data of Flaconnèche et al. at the same temperature. Similarly, our data at 50°C are close to the data of Flaconnèche et al. at 60°C. Carbon dioxide is also seen to be less soluble in the denser polymer.

At lower pressures, the solubility increases linearly with pressure (Henry's law behavior). However, at higher pressures, clear deviations from Henry's law behavior can be observed. Thus, the solubility of carbon dioxide in HDPE is well described by Henry's law up to the maximum experimental pressure of 40 bar.

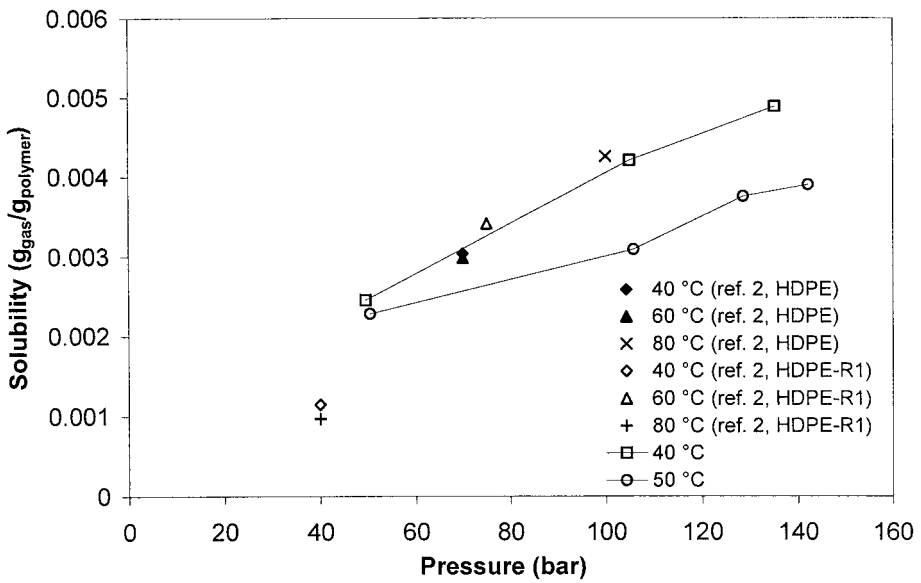

Figure 7 Solubility of methane in HDPE as a function of pressure. This plot compares the results of this study with those of Flaconnèche et al.[17]. The error bars have been left off this study's data points for clarity. The points are connected by lines to guide the eye.

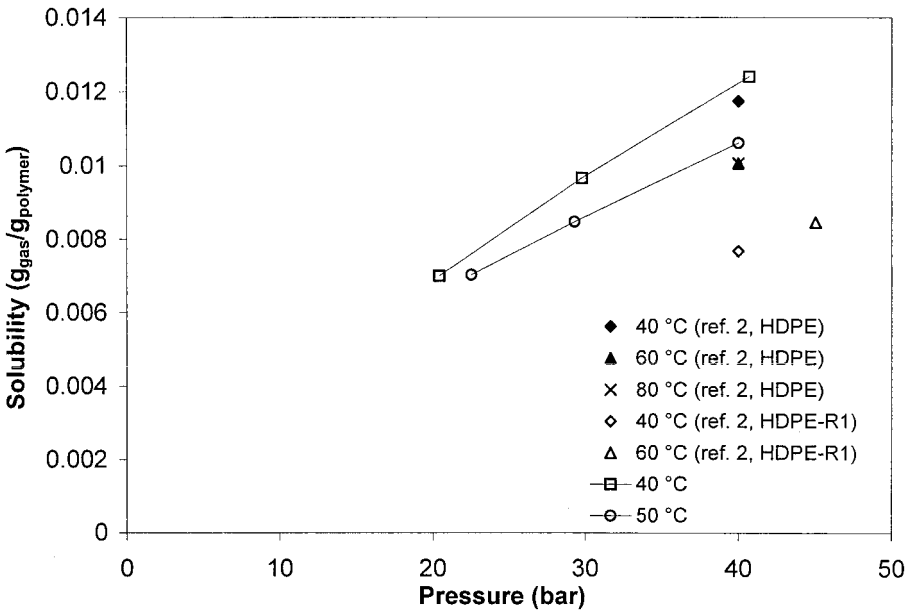

Figure 8 Solubility of carbon dioxide in HDPE as a function of pressure. This plot compares results of this study with those of Flaconnèche et al.[17]. The error bars have been left off this study's data points for clarity. The points are connected by lines to guide the eye.

For methane, negative deviations occur at high pressures (>100 bar). In this case, the data are best described by a so-called dual-mode adsorption mechanism,[18] which is a combination of Henry's law and Langmuir adsorption:

$$S = k_D P + \frac{C_H' b P}{1 + bP} \tag{5}$$

where S is the total equilibrium concentration (solubility) of the adsorbed gas, k_D is the Henry's law constant, P is the pressure, C_H' is the Langmuir capacity factor, and b is the Langmuir site affinity parameter. Figure 9 shows a plot of the solubility of methane in HDPE at 32°C predicted by a dual-mode adsorption mechanism, for which the parameters in eq. (5) have been fitted to the data. The contributions of the Henry's law and Langmuir portions are also shown. A pure Langmuir adsorption mechanism supposes the existence of vacancies in the polymer, which become filled with gas as the pressure is increased. Eventually, these vacancies become filled, and no further adsorption occurs as the pressure continues to increase. However, we observe that the solubility does increase, and this indicates that the superpositioning of Henry's law and Langmuir adsorption provides a more appropriate description of the data.

Figure 10 shows a pressurization experiment for carbon dioxide in HDPE at 39.1 bar and 25°C. In contrast to the methane experiments (see Fig. 2), there seem to be two processes occurring. A typical adsorption behavior is observed up to about 50 $s^{1/2}$. Thereafter, the mass appears to increase slowly up to about 200 $s^{1/2}$ before flattening out. This effect is most pronounced at the highest pressures at which the experiments were performed (ca. 40 bar), although it is evident to a lesser extent at the lower pressures as well. A possible explanation for this effect is swelling of the polymer. This process, which according to Figure 10 is slower than the diffusion process, has two effects. At first, the polymer swells. This reduction in the polymer density is perceived by the balance as a reduction in mass because of the increased buoyancy of the sample. However, the gas is then more soluble in the swollen polymer, and this results in an increase in the sample mass. Because the evacuation experiments (for which buoyancy is not a factor) give values similar to those from the pressurization experiments, we feel that any swelling that may occur will not significantly affect the solubility results obtained in our experiments. The solubility of carbon dioxide is generally rather low under these conditions (<1.5% of the polymer mass). Additionally, the reversibility of the experiment was confirmed by the repetition of the experiment under identical conditions, which yielded similar results for solubility. It is clear from Figure 10 that the final equilibrium solubility is attained much more slowly.

Diffusion coefficient

It is also possible to estimate diffusion coefficients from the measurements obtained from our apparatus. This information can be obtained from the way in

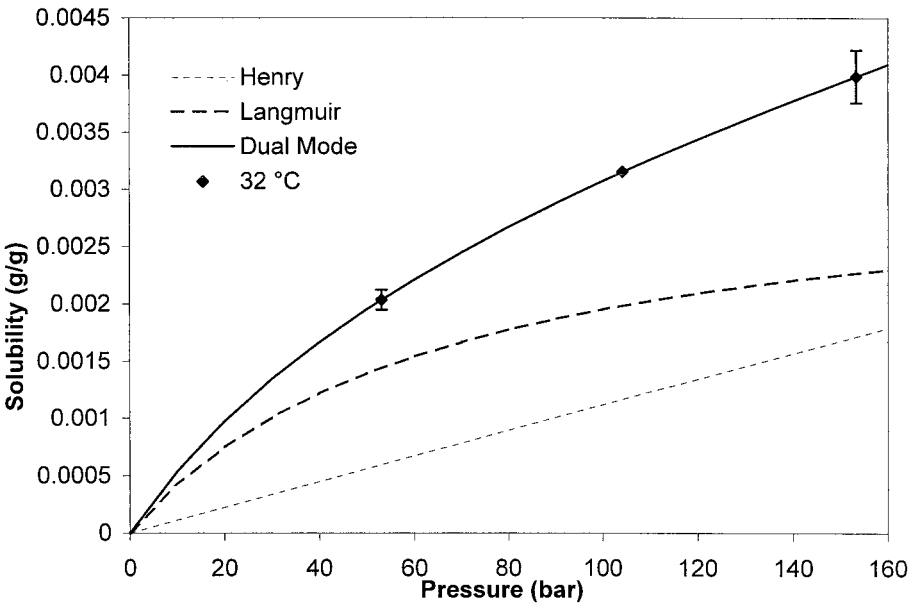

Figure 9 Solubility of methane in HDPE at 32°C as a function of pressure. The data are best described with a dual-mode adsorption mechanism. The contributions of the Henry's law portion and the Langmuir mechanism are also shown. The parameters in eq. (5) are $k_D = 1.12 \times 10^{-5}$ bar^{-1}, $C'_H = 3.27 \times 10^{-3}$ g of gas/g of polymer, and $b = 1.486 \times 10^{-2}$ bar^{-1}.

which the mass of the polymer increases with time as gas dissolves into it. To estimate the diffusion coefficient, we should account for the full geometry of the polymer discs in the calculation. The mass flux can be obtained from the solution to the diffusion equation for this geometry[19] by the combination of the solution for diffusion into a flat plate and into an infinitely long cylinder (both of these cases involve diffusion in one dimension). The solution for a cylinder of diameter a and height $2l$ is

$$\frac{M_t}{M_\infty} = 1 - \sum_{n=1}^{\infty} \frac{4}{a^2\alpha_n^2} e^{-D\alpha_n^2 t} \sum_{n=0}^{\infty} \frac{8}{(2n+1)^2\pi^2} e^{-D(2n+1)^2\pi^2 t/l^2} \tag{6}$$

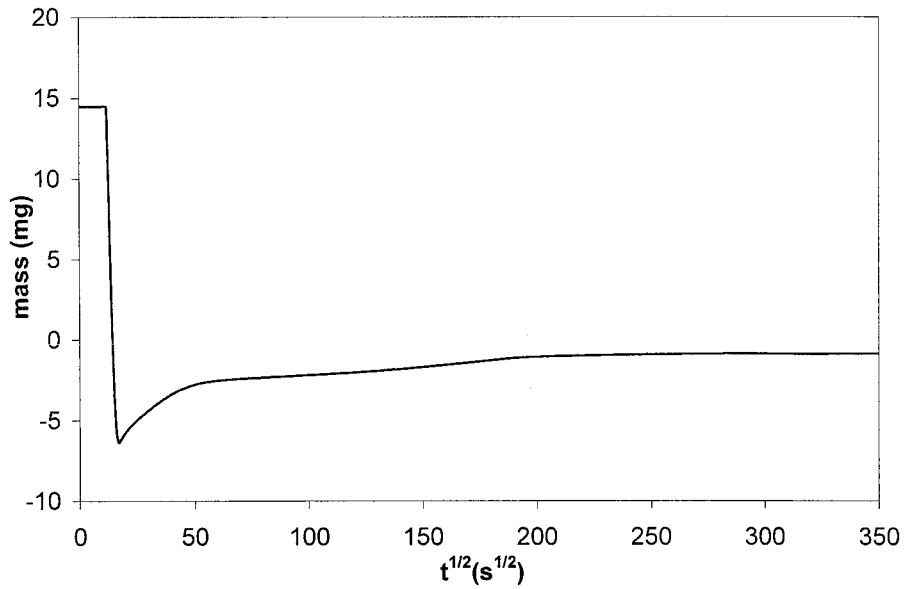

Figure 10 Pressurization experiment for carbon dioxide in HDPE at 39.1 bar and 25°C. The polymer mass is plotted against the square root of time. Two different processes seem to be occurring here. The expected adsorption curve occurs up to about 50 $s^{1/2}$, after which a gradual increase is observed up to about 200 $s^{1/2}$ before the curve becomes flat.

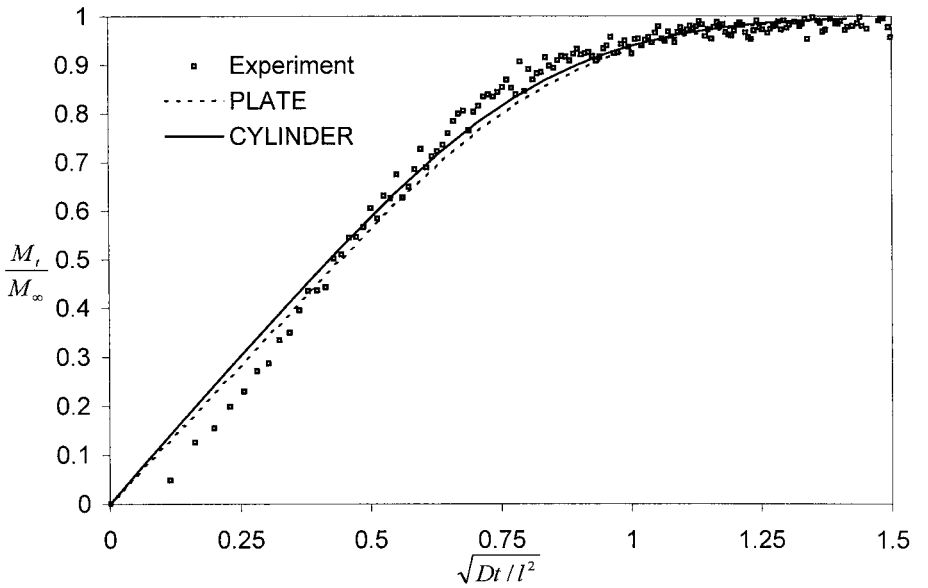

Figure 11 Generalized chart showing the ratio of the accumulated mass as a function of the square root of dimensionless time. The dotted line represents the solution assuming that the cylinder is a flat plate (no diffusion through the sides). The solid line represents the full solution assuming a cylinder diameter-to-height ratio of 20.2. The points are experimental data for methane at 157.1 bar and 32.1°C.

where α_n represents the positive solutions to the equation $J_0(a\alpha_n) = 0$ and J_0 is the Bessel function of the first kind of order zero. M_t is the mass of gas absorbed in time t, M_∞ is the mass absorbed at infinite time (the equilibrium value), and D is the diffusion coefficient. Figure 11 shows a generalized plot of M_t/M_∞ versus dimensionless time (the square root of Dt/l^2) for the case of a flat plate and for the geometry of the cylinders used in this study. The difference between the two is most apparent at short times, in the linear regime. In this regime, the solution for the full geometry predicts a mass absorbed that is greater than that of the flat plate by an amount equal to the extra area available for diffusion (the flat-plate solution ignores the area of the edge of the disc). This fact provides additional justification for the assumption discussed next.

Figure 12 shows the early part of the pressurization curve of Figure 2. Here the vertical axis has been normalized to show only the mass of gas accumulated. In the early part of the pressurization, the increase is linear with the square root of time. Following Cussler[20] for a semi-infinite medium, we have this relation:

$$Q = A\sqrt{\frac{4Dt}{\pi}}(c_{10} - c_{1\infty}) \tag{7}$$

where Q is the mass of gas accumulated (g), A is the area available for diffusion (cm^2), D is the diffusion coefficient (cm^2/s), and c_{10} and $c_{1\infty}$ are the concentrations at the interface and far from the interface, respectively. It is somewhat of a stretch to assume that the discs used in our measurements are semi-infinite plates; however, at very short times, this approximation is justified. The values of D are comparable to those obtained with the full analytical solution for this geometry [eq. (6)]. For the pressurization run shown in Figures 2 and 12, at short times, $c_{1\infty} = 0$ and $c_{10} = 0.00206$ g/cm^3 represent the driving force for diffusion, which is the saturation value of methane in this polymer (the measured solubility), that is, not the bulk gas concentration. The area available for diffusion is calculated as the total surface area of the eight polymer discs used in the experiment. The discs were assumed to have equal dimensions. An average disc was then assumed with a diameter of 10.31 mm (the thickness was measured to be 0.51 mm). Plotting Q against $t^{1/2}$ gives a straight line at short times, the slope of which gives D. For this particular case, we have obtained $D = 1.19 \times 10^{-7}$ cm^2/s. This is comparable to the value of 1.6×10^{-7} cm^2/s measured by Flaconnèche et al.[17] for a slightly less dense HDPE sample at 39°C.

Because of the uncertainty of diffusion coefficients measured in this way, it is generally felt that this method is not well suited to the measurement of diffusion coefficients. A possible source of uncertainty is the roughness of the polymer, which results in an estimate of the surface area available for diffusion that is too low, which, in turn, yields too high a diffusion coefficient. Another is the shape of the pieces used in the study (they are not that accurate); an average diameter was calculated on the basis of the total weight of the polymer, the number of discs, and the

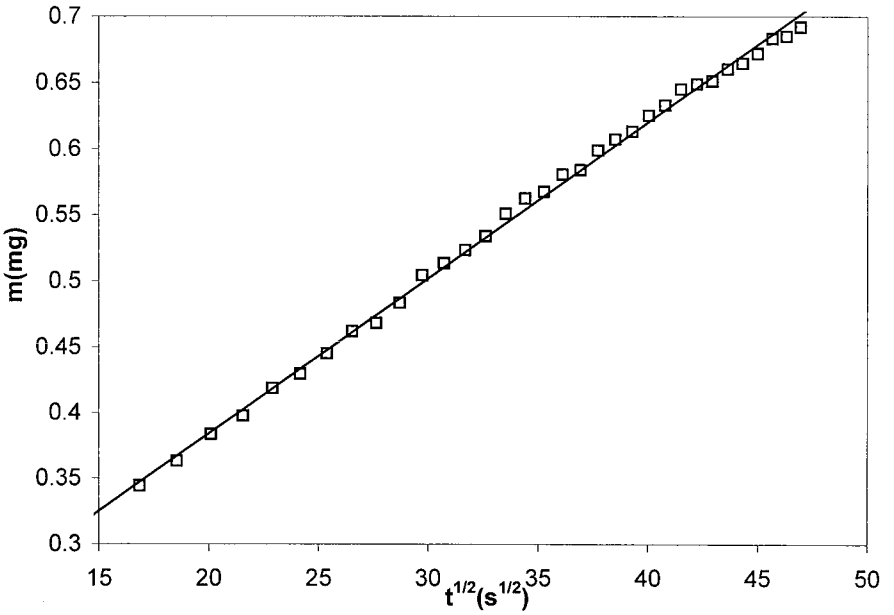

Figure 12 Mass of methane accumulated in HDPE as a function of the square root of time for short times. The points are data sampled during the run. The line is a linear fit of the data. The conditions are 32°C and 55.5 bar.

thickness. A further uncertainty comes from judging when the diffusion process is still in the linear regime. This can be partially eliminated by the minimization of the difference between the absorption plot obtained and that predicted based on theory for the exact geometry for the whole time period. However, this requires accurate measurements over the whole run. When fluctuations occur during the run, a better estimate of the diffusion coefficient is obtained with only data in the early (linear) part of the run. The values obtained are tabulated in Tables III and IV. Figures 13 and 14 show plots of the log of the diffusion coefficient as a function of the inverse temperature, averaged for all pressures. The expected linear (Arrhenius) trend is observed, although the large uncertainties in the method make any definite conclusions difficult. The problem of estimating when the diffusion process is still in the linear regime is exacerbated by the fact that the diffusion coefficient goes as the square of the slope [eq. (7)]. We consider our error in the estimation of the slope to be less than about 10%, and this means an error in the diffusion coefficient of about 20%. Additionally, it is evident from Figure 2 that the pressurization (or evacuation) process is not instantaneous but rather occurs over a period of about a minute. Hence, the start time of the diffusion process (t_0) is

TABLE III
Diffusivities of Methane in HDPE

25°C		32°C		40°C		50°C	
Pressure (bar)	Diffusivity (cm^2/s) $\times 10^7$	Pressure (bar)	Diffusivity (cm^2/s) $\times 10^7$	Pressure (bar)	Diffusivity (cm^2/s) $\times 10^7$	Pressure (bar)	Diffusivity (cm^2/s) $\times 10^7$
50.1	1.04	48.3	1.76	49.6	1.87	50.2	4.28
50.1	1.36	55.5	1.19	49.6	1.53	50.2	4.39
		55.5	2.17			50.9	3.87
						50.9	3.90
106	0.882	103.8	2.56	105	2.03	100.4	4.54
		105	2.68	105	2.16	105.4	4.59
						105.4	3.91
						106.3	3.61
142.2	1.15	150	0.987	135.2	2.08	142.2	3.63
142.2	1.14	151	1.11				
		151	2.15				
		157.1	1.43				
		157.1	2.84				

TABLE IV
Diffusivities of Carbon Dioxide in HDPE

25°C		32°C		40°C		50°C	
Pressure (bar)	Diffusivity (cm^2/s) $\times 10^7$	Pressure (bar)	Diffusivity (cm^2/s) $\times 10^7$	Pressure (bar)	Diffusivity (cm^2/s) $\times 10^7$	Pressure (bar)	Diffusivity (cm^2/s) $\times 10^7$
22.1	2.37	18.8	2.37	20.4	3.28	22.5	6.84
22.1	2.10	18.8	2.27			22.5	4.54
24	1.11						
24	2.20						
31.3	3.53	31.4	5.33	29.8	5.53	29.3	8.88
		31.4	2.43	29.8	4.08		
		31.6	6.26				
		31.6	4.20				
39.1	2.52	37.4	5.24	40.7	5.22	40	13.7
39.1	2.40	42.5	6.41			40	10.7
		42.5	5.76				

subject to some uncertainty because evidently diffusion starts to occur as soon as gas is introduced into the balance. Changing t_0 can change both the shape and the slope of the curve (plotting the mass vs the square root of time), although the error introduced in this way has been found to give an error in the diffusion coefficient of less than 5% for reasonable values of t_0.

CONCLUSIONS

Using a high-pressure microbalance, we have measured solubility and diffusion coefficients for the two gases methane and carbon dioxide in HDPE from 25 to 50°C and at pressures up to 150 bar. The polymer was cut from piping intended for use in offshore oil and gas applications. The method is well suited for determining the solubility of these gases in HDPE. Good agreement has been found with similar data for the same temperature and pressure ranges. The method can also be used to determine diffusion coefficients from the dynamic behavior of the system. However, the amount of scatter observed in the data suggests that the method is not well suited for this purpose.

In general, solubility data follow a Henry's law (linear) dependence on pressure, although at very high pres-

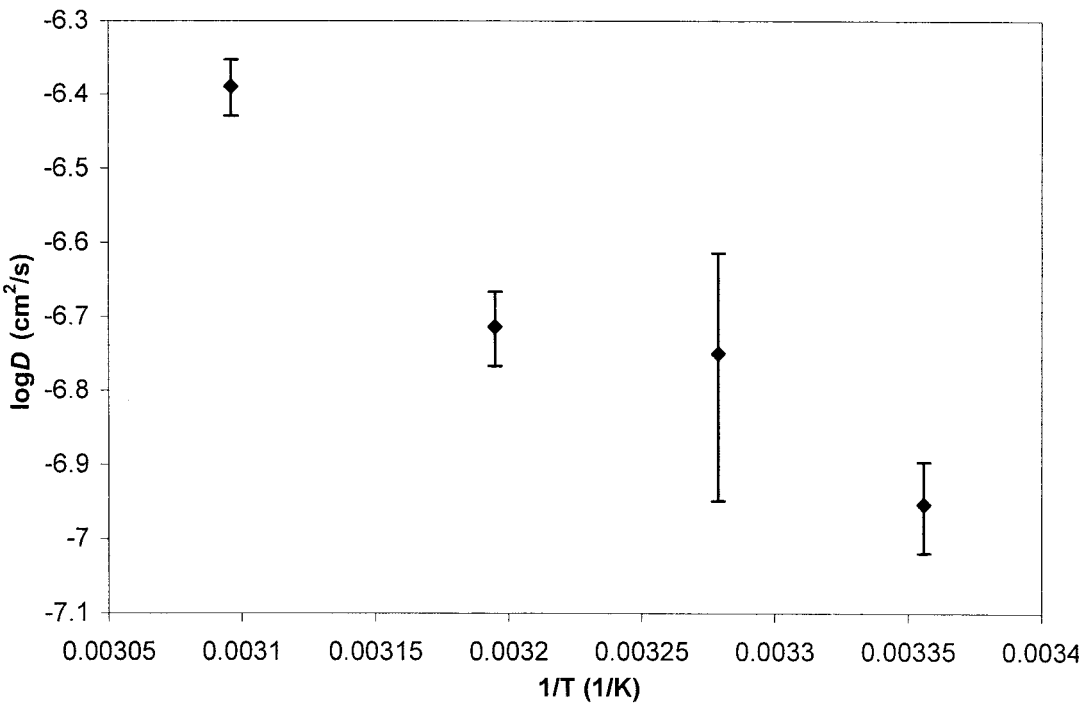

Figure 13 Log of the diffusion coefficient of methane as a function of the inverse temperature. The effect of the pressure on the diffusion coefficient was not measurable within the experimental uncertainty. The values have been averaged over all pressures at each temperature.

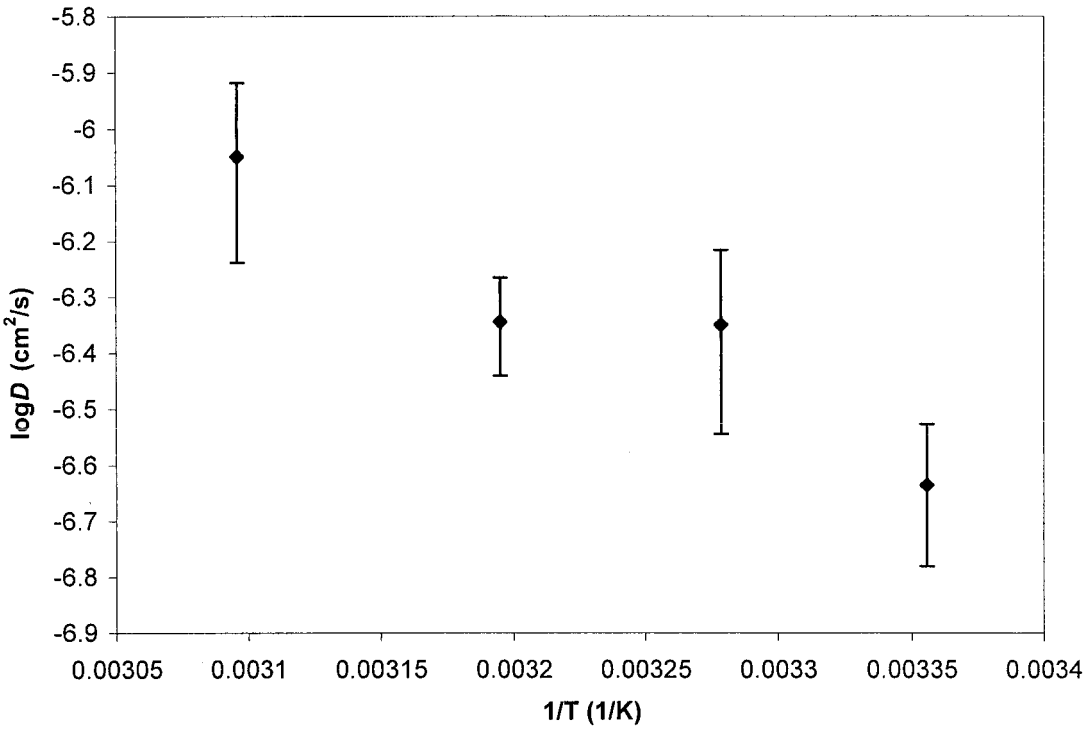

Figure 14 Log of the diffusion coefficient of carbon dioxide as a function of the inverse temperature. The effect of the pressure on the diffusion coefficient was not measurable within the experimental uncertainty. The values have been averaged over all pressures at each temperature.

sures, deviations from Henry's law have been observed. In this regime, a dual-mode adsorption mechanism is deemed a more appropriate description of the system.

The authors thank the following people who contributed to this work: Zacarias Tecle, Povl Valdemar Andersen, and Thuong Dang, for carrying out the majority of the experimental work; Jørgen Mollerup, for providing the computer program for the calculation of the gas P–v–T properties based on the Younglove and Ely[14] equation of state; Michael Michelsen, for providing the computer program used to calculate the solution to the diffusion equation for the finite cylinder geometry; Inger-Margrete Procida of NKT Flexibles (Brøndby, Denmark), for providing the polymer sheet and pipe samples as well as polymer data sheets; Alexander Shapiro, for helpful discussions concerning diffusion; and Georgios Kontogeorgis, for very useful discussions concerning polymer thermodynamics.

References

1. Jarrin, J. Oil Gas Sci Tech Rev IFP 2001, 56, 219.
2. Dawans, F.; Jarrin, J.; Hardy, J. SPE Prod Eng 1988, August, 387.
3. Klopffer, M. H.; Flaconnèche, B. Oil Gas Sci Tech Rev IFP 2001, 56, 223.
4. Morris, V. N.; Street, J. N. Ind Eng Chem 1929, 21, 1215.
5. van Amerongen, G. J. J Appl Phys 1946, 17, 972.
6. Michaels, A. S.; Parker, R. B., Jr. J Phys Chem 1958, 62, 1604.
7. Michaels, A. S.; Parker, R. B., Jr. J Polym Sci 1959, 41, 53.
8. Michaels, A. S.; Bixler, H. J. J Polym Sci 1961, 50, 393.
9. Michaels, A. S.; Bixler, H. J. J Polym Sci 1961, 50, 413.
10. Lowell, P. N.; McCrum, N. G. J Polym Sci Part A-2: Polym Phys 1971, 9, 1935.
11. Kulkarni, S. S.; Stern, S. A. J Polym Sci Polym Phys Ed 1983, 21, 441.
12. Aubert, J. H. J Supercrit Fluids 1998, 11, 163.
13. Webb, J. A.; Bower, D. I.; Ward, I. M.; Cardew, P. T. J Polym Sci Part B: Polym Phys 1993, 31, 743.
14. Younglove, B. A.; Ely, J. F. J Phys Chem Ref Data 1987, 16, 577.
15. Chau, C. C.; Raspor, O. C. J Polym Sci Part B: Polym Phys 1990, 28, 631
16. Crank, J.; Park, G. S. Diffusion in Polymers; Academic: New York, 1968.
17. Flaconnèche, B.; Martin, J.; Klopffer, M. H. Oil Gas Sci Tech Rev IFP 2001, 56, 261.
18. Pace, R. J.; Datyner, A. J Polym Sci Polym Phys Ed 1980, 18, 1103.
19. Crank, J. The Mathematics of Diffusion; Clarendon: Oxford, 1975.
20. Cussler, E. L. Diffusion–Mass Transfer in Fluid Systems; Cambridge University Press: Cambridge, England, 2000.